Article

Discovery Medicine 2026; 38(205): 443–452
https://doi.org/10.24976/Discov.Med.202638205.37

Propofol Ameliorates Neuroinflammation and Oxidative Stress in High-Fat Diet-Induced Rats via Regulation of the AMPK/mTOR Pathway

Siqi Ye[1,*], Ke Yan[1], Lei Li[1], Qiao Xu[1]

[1]Department of Anesthesiology, The Affiliated People's Hospital of Ningbo University, 315040 Ningbo, Zhejiang, China
*Correspondence: yzrm_ysq@163.com (Siqi Ye)
Submitted: 5 November 2025 Revised: 18 December 2025 Accepted: 7 January 2026 Published: 20 February 2026

Background: High-fat diet (HFD) induces neuroinflammation and oxidative stress, leading to cerebral injury and cognitive decline. Propofol, an intravenous anesthetic, exhibits anti-inflammatory and antioxidant effects. The present study aimed to evaluate its neuroprotective role in HFD-induced brain injury and to explore whether these effects may be associated with regulation of the AMP-activated protein kinase (AMPK)/mammalian target of rapamycin (mTOR) signaling pathway.
Methods: Rats were assigned to normal diet (ND), HFD, HFD+low-dose propofol, and HFD+high-dose propofol groups. After intervention, cognitive function was tested using the Morris water maze. Brain histopathology, apoptosis, inflammatory cytokines, oxidative stress markers, and protein expression related to apoptosis, autophagy, and AMPK/mTOR signaling were analyzed.
Results: HFD-fed rats exhibited impaired learning and memory performance, neuronal damage and apoptosis, increased levels of interleukin-1β (IL-1β), tumor necrosis factor-alpha (TNF-α), interleukin-6 (IL-6), and malondialdehyde (MDA), as well as reduced superoxide dismutase (SOD) activity and glutathione (GSH) levels (all $p < 0.05$), accompanied by autophagy dysregulation characterized by LC3-II accumulation and p62 upregulation, along with suppression of AMPK with activation of mTOR ($p < 0.05$). Propofol treatment, particularly at the higher dose, significantly improved cognitive function, attenuated neuronal injury and apoptosis, reduced inflammatory and oxidative stress markers, restored autophagy-related alterations, which were accompanied by enhanced AMPK activation and inhibited mTOR signaling ($p < 0.05$).
Conclusion: Propofol alleviates HFD-induced neuroinflammation, oxidative stress, apoptosis, and autophagy-related alterations, which may be associated with modulation of the AMPK/mTOR signaling pathway, supporting its potential as a therapeutic strategy for metabolic-associated neurological disorders.

Keywords: propofol; high-fat diet; AMPK/mTOR pathway; neuroinflammation; oxidative stress

Introduction

Obesity, driven largely by the widespread adoption of high-fat diets (HFD), has emerged as a significant global health concern, contributing not only to metabolic syndromes but also to central nervous system (CNS) dysfunction [1]. Accumulating evidence demonstrates that chronic HFD exposure induces neuroinflammation and oxidative stress, which are closely linked to cognitive deterioration and the pathogenesis of neurodegenerative disorders [2]. AMP-activated protein kinase (AMPK), along with the mammalian target of rapamycin (mTOR) signaling network, has been proven to be the core hub for the regulation of energy metabolism, inflammation and autophagy [3]. HFD-induced cerebral injury is increasingly recognized; however, the underlying mechanisms involving the AMPK/mTOR pathway remain poorly understood, and the feasibility of drug-based targeting of this pathway continues to pose significant challenges in current research.

HFD disrupts brain homeostasis through multiple pathways, involving key pathological processes such as oxidative stress, neuroinflammation, and programmed cell death disorder [4,5]. Excess lipid accumulation triggers the generation of reactive oxygen species (ROS) and upregulation of proinflammatory cytokines, leading to mitochondrial dysfunction and neuronal loss [6]. Dysregulated autophagy, a critical process for maintaining neuronal homeostasis, is commonly observed under metabolic stress conditions, which in turn exacerbates neurodegeneration [7].

Propofol, a widely used intravenous anesthetic, has gained attention for its potent anti-inflammatory and antioxidant properties in various models of brain injury [8,9]. Recent studies suggest that propofol can modulate autophagy and inhibit neuroinflammation, potentially through regulation of the AMPK/mTOR signaling cascade [10]. However, the precise mechanisms by which propofol ameliorates HFD-induced neuroinflammation and oxidative stress, particularly in relation to the AMPK/mTOR pathway, remain to be fully clarified.

This study explored the neuroprotective mechanisms of propofol and its regulatory effects on the AMPK/mTOR signaling pathway using an HFD-induced rat model, providing new insights into the therapeutic strategies for metabolism-linked neurodegenerative disorders.

Materials and Methods

Animal Modeling and Grouping

All experimental procedures were approved by the Institutional Animal Care and Use Committee of the Guangdong Provincial Medical Experimental Animal Center (IACUC Approval No. D202509-3) and were conducted in accordance with the ARRIVE guidelines. Twenty male Sprague–Dawley rats (6–8 weeks old, 250–300 g) were obtained from the Guangdong Provincial Medical Experimental Animal Center. Animals were housed under specific-pathogen-free (SPF) conditions in standard polycarbonate cages (3–5 rats per cage) at 22 ± 2 °C and 55 ± 10% relative humidity, with a 12/12 h light–dark cycle, and were provided food and water *ad libitum*. Following a 3–7-day acclimatization period, animals were randomly allocated into a normal diet control group (ND, n = 5) and a HFD modeling cohort (n = 15).

The HFD formula consists of 12% lard, 10% soybean oil, 20% sucrose, 15% egg yolk powder, 1% cholesterol, 0.5% sodium cholate, and 41.5% standard diet. Rats in the HFD and HFD+P groups were fed an HFD to induce obesity, while the ND group received a standard chow diet. Rats were fed the HFD for 8 weeks, after successful establishment of the HFD-induced obesity model was validated by body-weight assessment; rats exhibiting a ≥20% increase in body weight compared with age-matched ND controls were considered obese [2,11].

After confirmation of successful modeling, the HFD-fed rats were further randomly divided into three groups (n = 5 per group): HFD group, HFD plus low-dose propofol group (HFD+P-L), and HFD plus high-dose propofol group (HFD+P-H). Rats in the HFD+P-L and HFD+P-H groups were administered intraperitoneal injections of propofol (2078-54-8, MedChemExpress) at doses of 30 mg/kg and 60 mg/kg, respectively, for 8 weeks. The selected doses of propofol (30 and 60 mg/kg) were based on previous *in vivo* studies demonstrating their neuroprotective and anti-inflammatory effects without inducing excessive sedation or toxicity in rodent models [12,13]. The lower dose was chosen as a minimally effective concentration, whereas the higher dose was used to evaluate whether potential enhanced protective effects could be achieved within a safe pharmacological range. Rats in the ND and HFD groups received equivalent volumes of normal saline via intraperitoneal injection.

Cognitive Function Assessment

At the end of the intervention, cognitive function was evaluated using the Morris water maze test. Three days prior to the formal experiment, rats underwent environmental adaptation to the water maze, involving two daily 90-second habituation swims without platform placement, to familiarize them with the pool environment and swimming procedure. Water temperature was rigorously maintained consistent with laboratory ambient conditions. The formal protocol consisted of five consecutive days of place navigation trials, followed by a spatial probe test on day 6. During the place-navigation phase, each rat underwent four training trials daily for five consecutive days. Escape latency (s) was recorded in each trial to measure spatial learning. Rats were released from randomly chosen start points and allowed up to 90 seconds to locate the hidden platform. If a rat failed to find the platform within this time, it was guided to the platform and remained there for 15 seconds. For the spatial probe, the test was performed by removing the platform and introducing the rat into the pool from a random quadrant. The number of platform crossings and the time spent in the target quadrant were recorded as indices of memory retention. Animal movement trajectories and behavioral parameters were recorded and analyzed using an automated video tracking system (ANY-maze Video Tracking System, version 6.33, Stoelting Co., Wood Dale, IL, USA).

Histopathological and Histological Analysis

Following behavioral testing, rats were deeply anesthetized using 5% isoflurane inhalation and euthanized by cervical dislocation under deep anesthesia, in accordance with institutional and ARRIVE guidelines. Death was confirmed by the absence of heartbeat, respiration, corneal reflex, and response to toe pinch, after which their brain tissues were collected. Part of the tissue samples was rapidly cryopreserved in liquid nitrogen at –80 °C for further analysis, while the remaining samples were fixed in 4% paraformaldehyde and preserved at 4 °C. Subsequently, the fixed samples underwent a series of dehydration procedures and were embedded in paraffin to prepare histological sections. All histological and immunohistochemical evaluations, including hematoxylin and eosin (H&E) staining, Nissl staining, TUNEL staining, and immunohistochemical staining, were performed on sections obtained from the hippocampal region of the rat brain.

Paraffin sections were routinely processed for H&E staining using a HE Staining Kit (G1005, Servicebio, Wuhan, China) to evaluate general histopathological changes under light microscopy. Nissl staining using cresyl violet was performed with a Nissl Staining Kit (G1036, Servicebio, Wuhan, China) to assess neuronal survival and morphological integrity. TUNEL staining was conducted using a TUNEL Apoptosis Detection Kit (C1088, Beyotime Biotechnology, Shanghai, China) to detect apoptotic cells, with nuclei counterstained by DAPI (C1002, Beyotime

Biotechnology, Shanghai, China). In addition, immunohistochemical staining was performed to examine the expression and distribution of AMPK, p-AMPK, mTOR, and p-mTOR using the following primary antibodies: AMPK (rabbit polyclonal, ab32047, 1:200, Abcam, Cambridge, UK), p-AMPK (rabbit monoclonal, #2535, 1:200, Cell Signaling Technology, Danvers, MA, USA), mTOR (rabbit monoclonal, #2983, 1:200, Cell Signaling Technology, Danvers, MA, USA), and p-mTOR (rabbit monoclonal, #2976, 1:100, Cell Signaling Technology, Danvers, MA, USA). Immunoreactivity was visualized using diaminobenzidine (DAB), and quantitative analysis was conducted by measuring the integrated optical density (IOD) per area using ImageJ software (version 1.53, National Institutes of Health, Bethesda, MD, USA).

Biochemical Analysis

Brain tissue homogenates were prepared for enzyme-linked immunosorbent assay (ELISA) to quantify inflammatory cytokines interleukin-1β (IL-1β), tumor necrosis factor-alpha (TNF-α), and interleukin-6 (IL-6) using commercial ELISA kits (IL-1β: E-EL-R0012; TNF-α: E-EL-R2856; IL-6: E-EL-R0015, Elabscience Biotechnology Co., Ltd., Wuhan, China). Briefly, frozen brain tissues were homogenized in ice-cold phosphate-buffered saline and centrifuged at 12,000 $\times$g for 10 min at 4 °C, and the supernatants were collected for analysis. ELISA measurements were performed using a microplate reader (Synergy™ H1, BioTek Instruments, Winooski, VT, USA) at a wavelength of 450 nm. Cytokine concentrations were calculated from standard curves and normalized to total protein content.

Oxidative stress markers, including superoxide dismutase (SOD) activity, malondialdehyde (MDA) content, and glutathione (GSH) levels, were also assessed using commercial assay kits (SOD: S0101M, MDA: S0131M; GSH: S0052, Beyotime Biotechnology, Shanghai, China) according to the manufacturers' protocols. Absorbance values were measured using the same microplate reader at the recommended wavelengths, and results were quantified based on standard curves or calculation formulas provided by the manufacturers.

Western Blotting

Protein extracts from brain tissues were subjected to Western blotting to determine the expression levels of apoptosis-related proteins (Bax, Bcl-2, cleaved caspase-3), autophagy markers (LC3-II/LC3-I ratio, p62), and key proteins in the AMPK/mTOR signaling pathway (phosphorylated AMPK [p-AMPK], total AMPK, phosphorylated mTOR [p-mTOR], and total mTOR). Briefly, total protein was extracted using RIPA lysis buffer supplemented with protease and phosphatase inhibitors, and protein concentrations were determined using a BCA assay. Equal amounts of protein (30 µg) were separated by SDS–PAGE and transferred onto PVDF membranes. Membranes were blocked with 5% non-fat milk in TBST for 1 h at room temperature and incubated with primary antibodies overnight at 4 °C. The following primary antibodies were used: Bax (ab32503, rabbit, 1:1000, Abcam, Cambridge, UK), Bcl-2 (ab194583, rabbit, 1:1000, Abcam, Cambridge, UK), cleaved caspase-3 (9661, rabbit, 1:1000, Cell Signaling Technology, Danvers, MA, USA), LC3B (2775, rabbit, 1:1000, Cell Signaling Technology, Danvers, MA, USA), p62 (5114, rabbit, 1:1000, Cell Signaling Technology, Danvers, MA, USA), p-AMPK (Thr172) (2535, rabbit, 1:1000, Cell Signaling Technology, Danvers, MA, USA), AMPK (2532, rabbit, 1:1000, Cell Signaling Technology, Danvers, MA, USA), p-mTOR (Ser2448) (5536, rabbit, 1:1000, Cell Signaling Technology, Danvers, MA, USA), mTOR (2983, rabbit, 1:1000, Cell Signaling Technology, Danvers, MA, USA), and β-actin (8457, rabbit, 1:2000, Cell Signaling Technology, Danvers, MA, USA). After washing, membranes were incubated with HRP-conjugated secondary antibody (7074, goat anti-rabbit IgG, 1:5000, Cell Signaling Technology, Danvers, MA, USA) for 1 h at room temperature. Protein bands were visualized using enhanced chemiluminescence and quantified by densitometry, normalized to β-actin as loading controls. Chemiluminescent signals were detected using a ChemiDoc XRS+ imaging system (Bio-Rad, Hercules, CA, USA), and band intensities were quantified using ImageJ software (National Institutes of Health, Bethesda, MD, USA).

Statistical Analysis

SPSS v26.0 (version 26.0, IBM Corp., Armonk, NY, USA) served as the statistical software. Results were expressed as mean $\pm$ standard deviation (SD). Statistical comparisons across the four groups were performed via one-way analysis of variance (ANOVA), accompanied by Tukey's post hoc for multiple testing. Significance was set at $p < 0.05$. For all evaluations, data normality was examined through the Shapiro–Wilk test, and variance homogeneity was determined by Levene's test. If parametric assumptions were not satisfied, the Kruskal–Wallis nonparametric test was used, with Dunn's post hoc procedure for multiple comparisons.

Results

Propofol Improves Cognitive Function in HFD-Induced Obese Rats

Using the Morris water maze, we conducted testing to determine the influence of propofol on spatial cognition in HFD-fed rats. Fig. 1A illustrates that, relative to the ND group, rats fed the HFD exhibited markedly prolonged escape latency during the acquisition phase ($p < 0.05$), indicating impaired learning ability. Treatment with propofol at both low and high doses (HFD+P-L and HFD+P-H groups) markedly shortened escape latency compared to the HFD

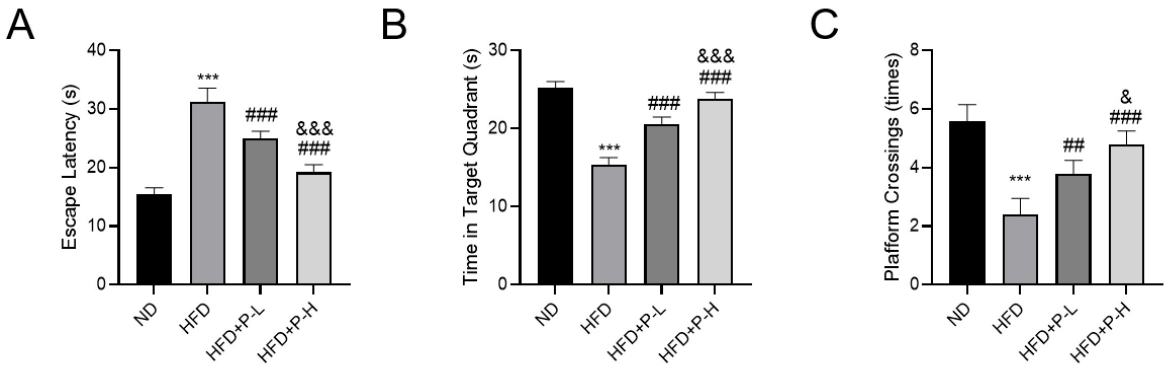

Fig. 1. Propofol's impact on cognitive performance in HFD-fed rats assessed by the Morris water maze. (A) Escape latency during acquisition across different groups. (B) Target quadrant occupancy. (C) Platform crossing frequency in the probe test. n = 5, $^{***}p < 0.001$ vs. ND, $^{\#\#}p < 0.01$, $^{\#\#\#}p < 0.001$ vs. HFD, $^{\&}p < 0.05$, $^{\&\&\&}p < 0.001$ vs. HFD+P-L. HFD, high-fat diet; ND, normal diet.

group (all $p < 0.05$), with the high-dose group showing more pronounced improvement ($p < 0.05$). In the probe trial (Fig. 1B,C), HFD rats exhibited less occupancy in the target quadrant and performed fewer crossings of the platform than ND rats ($p < 0.05$). Propofol administration significantly resulted in greater occupancy of the target quadrant and more platform crossings relative to HFD rats ($p < 0.05$), suggesting amelioration of memory deficits.

Propofol Can Alleviate the Histopathological Damage and Apoptosis of Brain Tissue

To evaluate the protective role of propofol on brain histopathology and neuronal apoptosis, H&E staining, TUNEL assay, and Nissl staining were performed. As shown in Fig. 2A, H&E staining demonstrated that neurons within the ND group were arranged orderly with clear nuclei and intact morphology. In contrast, the HFD group showed disorganized neuronal arrangement, nuclear pyknosis, and infiltration of inflammatory cells, indicating neuroinflammation and neuronal injury. Both propofol-treated groups exhibited significant attenuation of these pathological changes, with reduced neuronal damage and inflammatory infiltration compared to the HFD group. TUNEL staining revealed a significantly increased apoptosis rate among HFD rats compared to ND controls ($p < 0.05$), whereas propofol administration significantly reduced neuronal apoptosis, as evidenced by the lower number of TUNEL-positive cells (Fig. 2B). Notably, the high-dose propofol group showed a more pronounced anti-apoptotic effect ($p < 0.05$). Nissl staining further demonstrated that the count of Nissl-positive neurons was markedly decreased within the HFD group ($p < 0.05$), indicating extensive neuronal loss or damage. Propofol treatment significantly restored the number of Nissl-stained neurons, with greater improvement observed in the HFD+P-H group (all $p < 0.05$) (Fig. 2C), suggesting that propofol effectively attenuates neuronal injury and supports neuronal survival under HFD-induced stress.

Propofol Reduces Neuroinflammation and Oxidative Stress Markers

To investigate the effects of propofol on neuroinflammation and oxidative stress in rats subjected to an HFD, the levels of inflammatory cytokines and oxidative stress markers in brain tissues were examined. ELISA results demonstrated that levels of pro-inflammatory cytokines IL-1β, TNF-α, and IL-6 in brain tissues were notably elevated within the HFD group relative to ND controls ($p < 0.05$). Propofol administration significantly reduced the levels of pro-inflammatory cytokines compared with the HFD group; notably, a significantly greater reduction in TNF-α and IL-6 levels was observed in the HFD+P-H group than in the HFD+P-L group ($p < 0.05$), whereas no significant difference was detected between the two doses for IL-1β (Fig. 3A–C). Regarding oxidative stress indicators, as shown in Fig. 3D–F, HFD rats showed a marked reduction in SOD activity and GSH content, along with increased MDA levels (all $p < 0.05$). Propofol administration reversed these changes, significantly enhancing antioxidant enzyme activity and reducing lipid peroxidation ($p < 0.05$).

Propofol Modulates Apoptosis-Related Protein Expression

To further elucidate the molecular mechanisms underlying propofol's neuroprotective effects, the expression of apoptosis-related proteins was assessed by Western blotting. Fig. 4A–E demonstrates that the HFD group exhibited significantly decreased expression of the anti-apoptotic protein Bcl-2 and markedly increased levels of pro-apoptotic proteins (Bax, cleaved caspase-3, and cleaved PARP) compared with the ND group ($p < 0.05$), indicating enhanced neuronal apoptosis. Treatment with propofol at both low and high doses significantly reversed these changes. Specifically, propofol administration upregulated Bcl-2 expression while downregulating the pro-apoptotic proteins relative to the HFD group ($p < 0.05$). The HFD+P-H group exhibited more pronounced effects ($p < 0.05$), suggesting differential effects between the two tested doses.

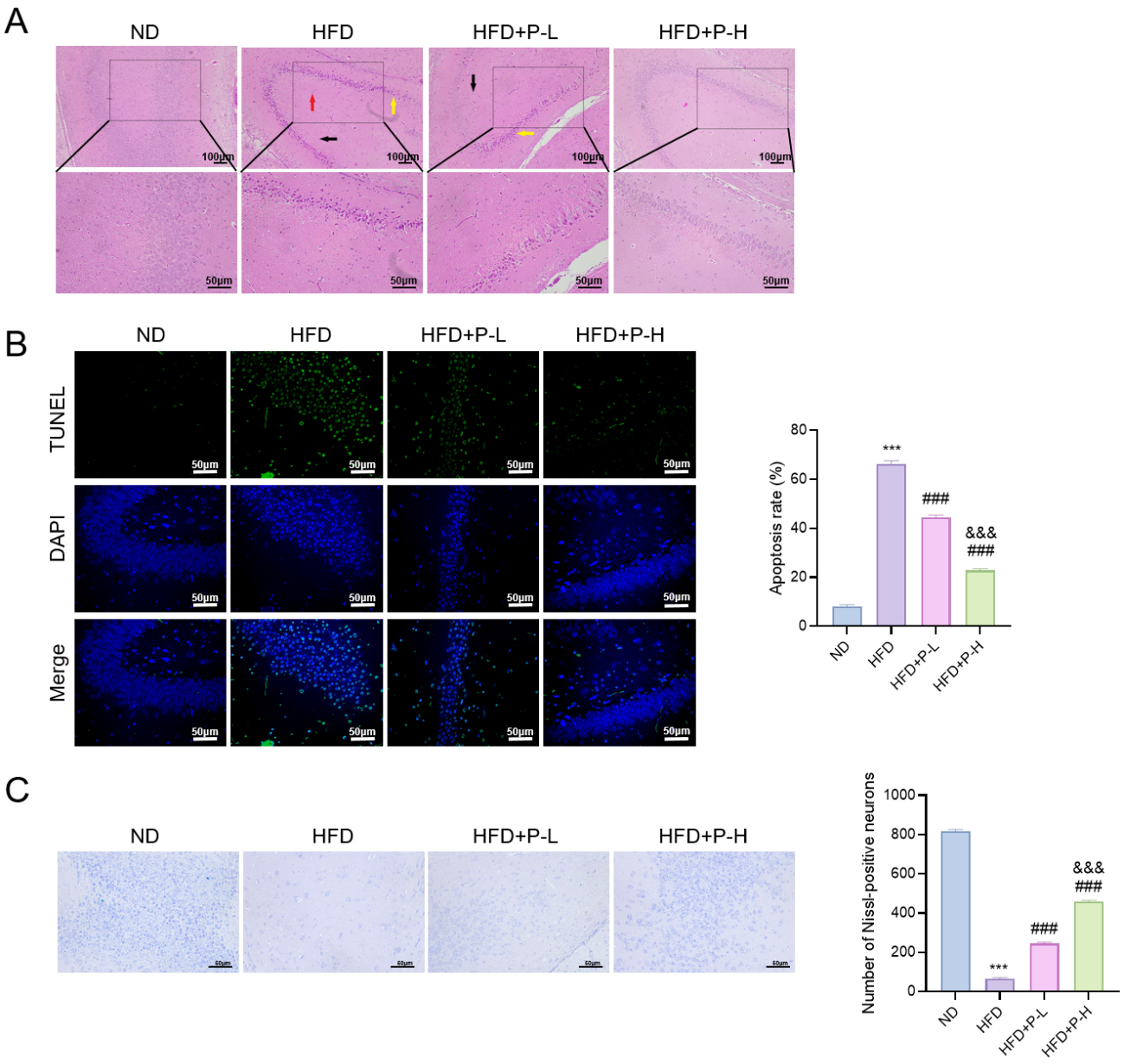

Fig. 2. Propofol alleviates histopathological damage and neuronal apoptosis in the brains of HFD-fed rats. (A) Representative images of H&E-stained brain tissue sections. Black arrows indicate disorganized neuronal arrangement and neuronal loss; red arrow indicates nuclear pyknosis; yellow arrows indicate inflammatory cell infiltration. (B) TUNEL assay showing apoptotic cells (green) and DAPI-stained nuclei (blue). Quantitative analysis of the apoptosis rate is shown on the right. (C) Nissl staining of brain sections. Quantification of Nissl-positive neuron numbers is shown on the right. n = 5, $^{***}p < 0.001$ vs. ND; $^{\#\#\#}p < 0.001$ vs. HFD, $^{\&\&\&}p < 0.001$ vs. HFD+P-L. H&E, hematoxylin and eosin; TUNEL, terminal deoxynucleotidyl transferase–mediated dUTP nick end labeling; DAPI, 4′,6-diamidino-2-phenylindole.

Impaired Autophagy in HFD-Fed Rats Is Reversed by Propofol Treatment

To determine whether propofol modulates autophagy in the context of high-fat diet (HFD)-induced brain dysfunction, the expression levels of autophagy-related markers LC3 and p62 were assessed by Western blotting. As shown in Fig. 5, compared with the ND group, rats in the HFD group exhibited a significantly increased LC3-II/LC3-I ratio, accompanied by a marked upregulation of p62 expression ($p < 0.05$), indicating autophagy dysregulation characterized by LC3-II accumulation and impaired autophagic flux. Treatment with propofol at both low and high doses significantly attenuated these alterations. Specifically, propofol administration significantly decreased p62 expression relative to the HFD group, whereas the LC3-II/LC3-I ratio was significantly reduced only in the HFD+P-H group ($p < 0.05$). These findings suggest a partial alleviation of HFD-induced abnormal autophagy status. The

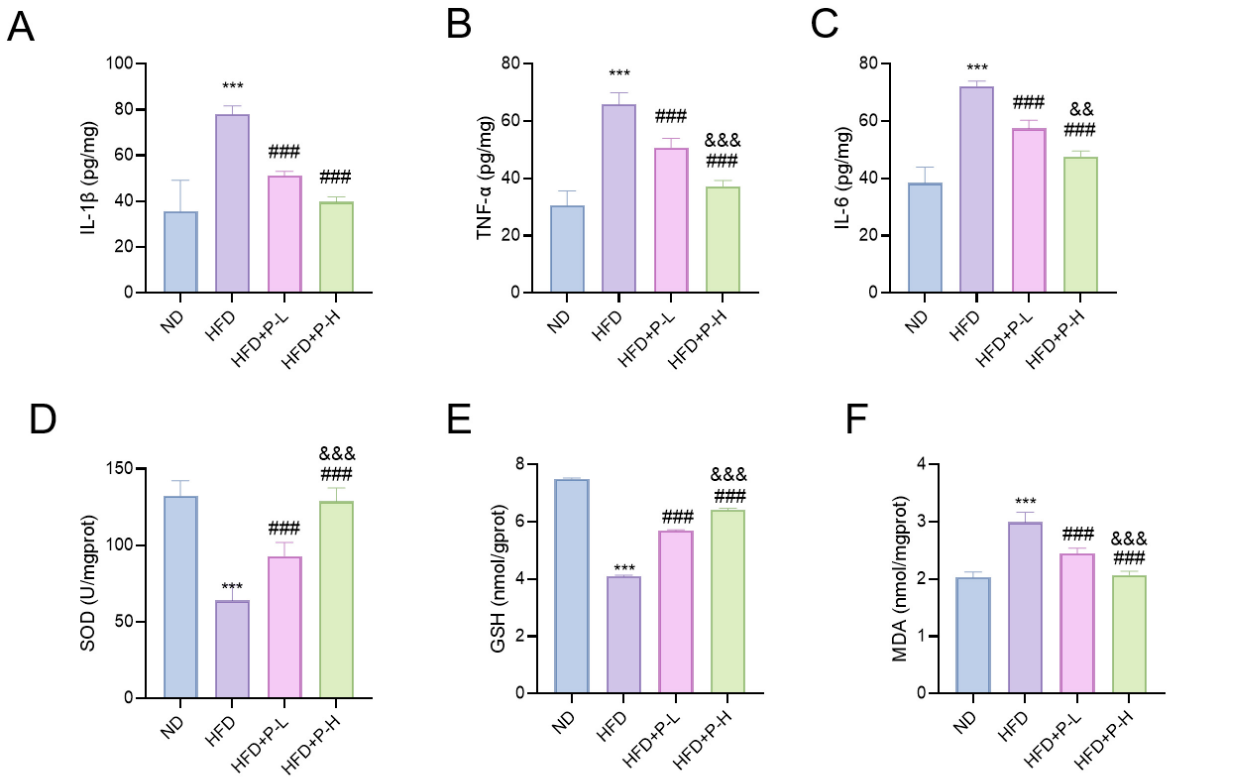

Fig. 3. Analysis of inflammatory cytokines and oxidative stress markers in brain samples from rats subjected to different dietary conditions. (A–C) IL-1β, TNF-α, and IL-6 quantified by ELISA. (D) SOD activity in brain tissues for each group. (E) Brain GSH concentration. (F) MDA levels in brain tissues. n = 5, $^{***}p < 0.001$ vs. ND, $^{\#\#\#}p < 0.001$ vs. HFD, $^{\&\&}p < 0.01$, $^{\&\&\&}p < 0.001$ vs. HFD+P-L. IL-1β, interleukin-1β; TNF-α, tumor necrosis factor-alpha; IL-6, interleukin-6; ELISA, enzyme-linked immunosorbent assay; SOD, superoxide dismutase; GSH, glutathione; MDA, malondialdehyde.

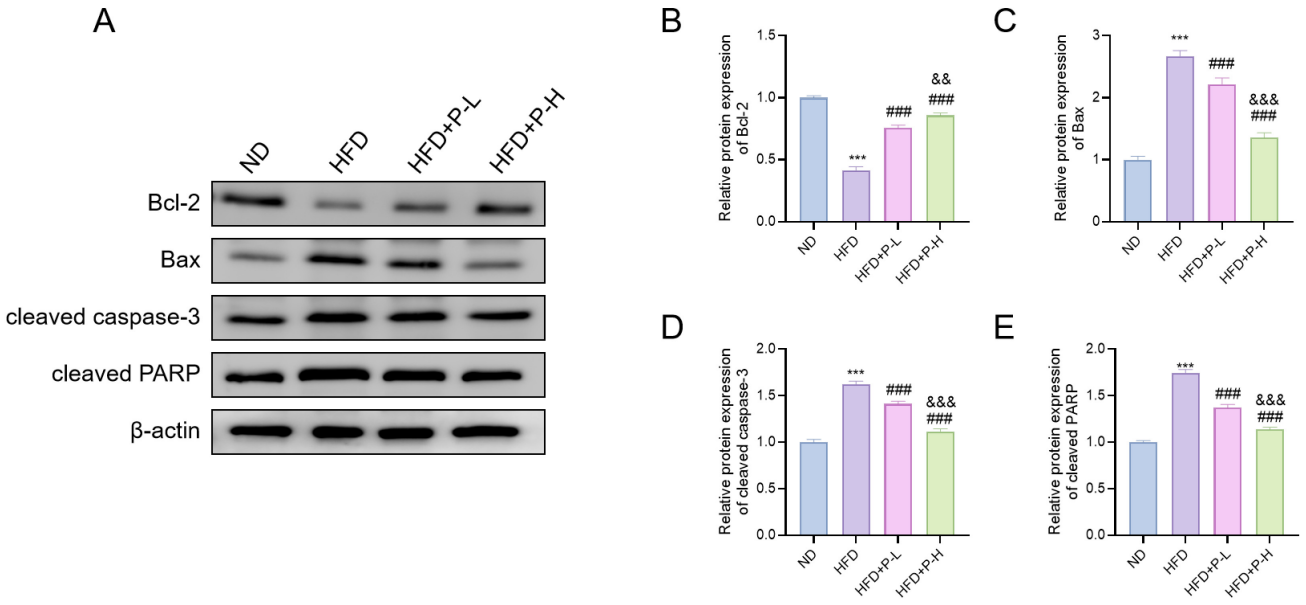

Fig. 4. Propofol modulates the expression of apoptosis-associated proteins within brain tissues from HFD-fed rats. (A) Representative Western blotting images. (B–E) quantification of relative protein levels (right) for Bcl-2, Bax, cleaved caspase-3, and cleaved PARP in brain tissues across ND, HFD, HFD+P-L, and HFD+P-H groups. β-actin was applied as the loading reference. n = 3, $^{***}p < 0.001$ vs. ND; $^{\#\#\#}p < 0.001$ vs. HFD, $^{\&\&}p < 0.01$, $^{\&\&\&}p < 0.001$ vs. HFD+P-L. Bcl-2, B-cell lymphoma 2; Bax, Bcl-2–associated X protein; PARP, poly(ADP-ribose) polymerase.

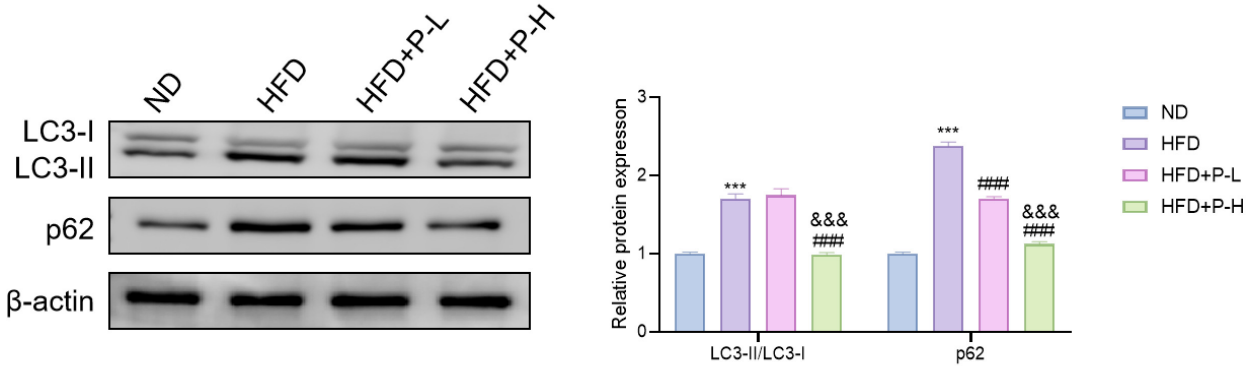

Fig. 5. Propofol restores autophagy markers in HFD-fed rat brains. Western blot images (left) and quantification (right) of LC3-I, LC3-II, and p62 across ND, HFD, HFD+P-L, and HFD+P-H groups. The LC3-II/LC3-I ratio indicated autophagic activity, while p62 accumulation reflected impairment. n = 3, $^{***}p < 0.001$ vs. ND; $^{\#\#\#}p < 0.001$ vs. HFD, $^{\&\&\&}p < 0.001$ vs. HFD+P-H. LC3, microtubule-associated protein 1 light chain 3.

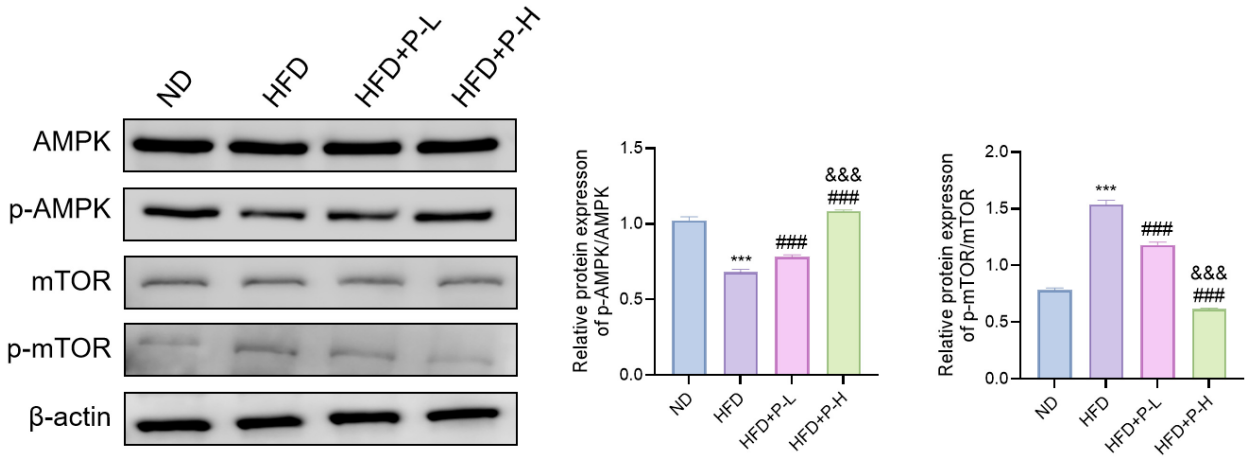

Fig. 6. Propofol regulates the AMPK/mTOR signaling pathway in HFD-fed rat brains. Western blotting and densitometric analysis of phosphorylated and total AMPK (top panel) and mTOR (bottom panel) in the ND, HFD, HFD+P-L, and HFD+P-H groups; β-actin was applied as the loading control. n = 3, $^{***}p < 0.001$ vs. ND; $^{\#\#\#}p < 0.001$ vs. HFD, $^{\&\&\&}p < 0.001$ vs. HFD+P-L. AMPK, AMP-activated protein kinase; p-AMPK, phosphorylated AMPK; mTOR, mammalian target of rapamycin; p-mTOR, phosphorylated mTOR.

HFD+P-H group showed a more pronounced normalization of LC3-II/LC3-I and p62 levels compared with the HFD+P-L group. Collectively, these results indicate that propofol mitigates HFD-induced autophagy dysregulation and contributes to the restoration of autophagy homeostasis.

Propofol Reverses High-Fat Diet–Induced Dysregulation of AMPK and mTOR Signaling in Brain Tissue

To investigate the involvement of AMPK/mTOR signaling in propofol-induced neuroprotection, phosphorylation changes of AMPK and mTOR in brain tissues were examined. According to Fig. 6, AMPK phosphorylation levels (p-AMPK/AMPK ratio) were significantly decreased in the HFD group compared to the ND group ($p < 0.05$). Propofol treatment significantly increased AMPK phosphorylation, with a greater effect observed in the high-dose group ($p < 0.05$). In contrast, the phosphorylation of mTOR (p-mTOR/mTOR ratio) was markedly elevated in the HFD group ($p < 0.05$), indicating overactivation of mTOR signaling. Propofol administration significantly reduced mTOR phosphorylation compared with the HFD group, with a significantly greater reduction observed in the HFD+P-H group than in the HFD+P-L group ($p < 0.05$). These findings suggest that propofol may attenuate neuronal injury and be associated with improvement of autophagy-related alterations, potentially involving modulation of the AMPK/mTOR signaling pathway.

Propofol Modulates AMPK/mTOR Signaling Pathway in Brain Tissue of HFD-Fed Rats

To further verify the regulatory effects of propofol on AMPK/mTOR signaling at the tissue level, immunohistochemical staining was performed to detect the expression and distribution of AMPK, p-AMPK, mTOR, and p-mTOR in rat brain tissues. As shown in Fig. 7, compared

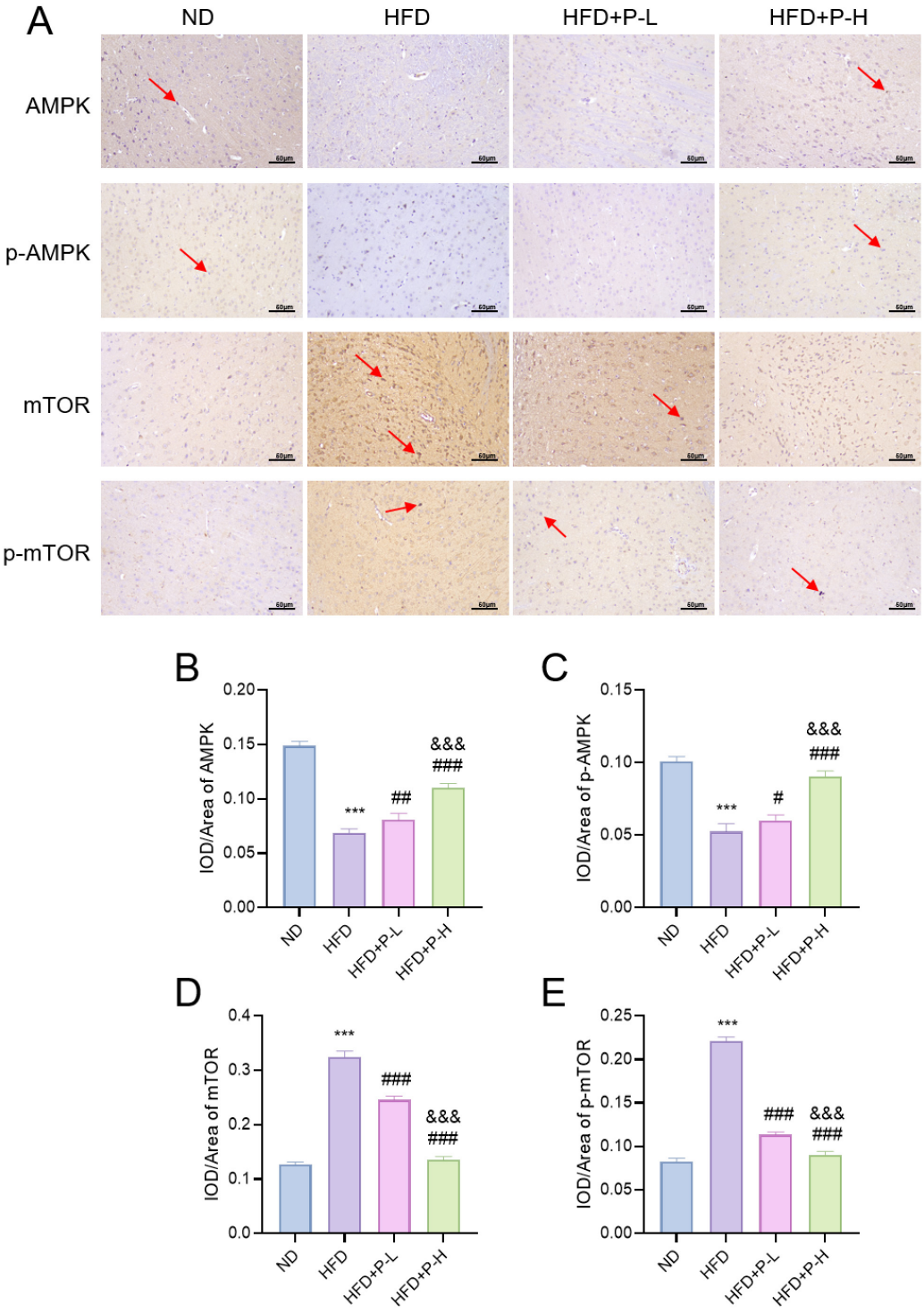

Fig. 7. Propofol alters the expression and distribution of AMPK/mTOR signaling proteins in rat brain tissue. (A) Representative immunohistochemical staining images of AMPK, p-AMPK, mTOR, and p-mTOR in brain tissues from the ND, HFD, HFD+P-L, and HFD+P-H groups. Red arrows indicate areas with positive immunoreactivity. (B–E) Quantification of integrated optical density (IOD) per area for AMPK (B), p-AMPK (C), mTOR (D), and p-mTOR (E). n = 5, $^{***}p < 0.001$ vs. ND; $^{\#}p < 0.05$, $^{\#\#}p < 0.01$, $^{\#\#\#}p < 0.001$ vs. HFD, $^{\&\&\&}p < 0.001$ vs. HFD+P-L. AMPK, AMP-activated protein kinase; p-AMPK, phosphorylated AMPK; mTOR, mammalian target of rapamycin; p-mTOR, phosphorylated mTOR.

with the ND group, rats in the HFD group showed notably reduced immunoreactivity for AMPK and p-AMPK ($p < 0.05$), indicating suppression of AMPK signaling. In contrast, mTOR and p-mTOR expression was markedly ele-

vated in the HFD group ($p < 0.05$), suggesting excessive activation of mTOR signaling. Propofol treatment at both low and high doses restored the AMPK/p-AMPK levels and reduced mTOR/p-mTOR levels relative to the HFD group ($p < 0.05$), with the HFD+P-H showing more pronounced effects ($p < 0.05$). These results further support the role of AMPK/mTOR signaling in propofol-modulated neuroprotection.

Discussion

This investigation demonstrated that propofol treatment significantly ameliorated HFD-induced neuroinflammation and oxidative stress in rat brain tissue. Our findings revealed that propofol exerted protective effects that were associated with AMPK activation, together with mTOR suppression. Specifically, propofol treatment reversed HFD-induced elevation of inflammatory cytokines, restored antioxidant capacity, reduced apoptosis markers, and normalized autophagy-related alterations. These findings indicate that propofol could represent a potential treatment for metabolism-related neurological disorders.

Previous studies have demonstrated that HFD-induced obesity exerts negative impacts on brain function [14,15], a finding that is further supported by the present study. Specifically, the Morris water maze assay, a widely recognized tool for assessing spatial learning and memory, revealed significant cognitive impairments in rats subjected to an HFD regimen. The observed decline in cognitive function is likely to be a consequence of neuroinflammation and oxidative stress, both of which are known to be triggered by HFD [16]. In the context of this study, the administration of propofol treatment led to a marked improvement in these symptoms. This improvement suggests that propofol may possess neuroprotective properties, potentially acting by alleviating the adverse effects of HFD on cognitive performance.

Autophagy is a highly conserved cellular degradation process involving lysosomal degradation for the renewal of proteins, protein complexes, and organelles [17]. Impairments in autophagy have been shown to disrupt intercellular communication and are associated with pathological conditions, including neurodegenerative diseases [18]. It has been demonstrated that the AMPK/mTOR signaling pathway can induce autophagy [19,20]. Cheng *et al.* [21] found that autophagy mediated by the AMPK/mTOR signaling pathway exerts neuroprotective effects in mice. Moreover, as a widely used intravenous anesthetic, propofol has garnered increasing attention for its potential role in modulating autophagy across various disease models [13]. In our HFD-induced obese rats, histopathological analysis revealed significant neuronal injury accompanied by neuroinflammation, along with evidence of autophagy dysregulation and altered AMPK/mTOR pathway activity. Propofol treatment attenuated HFD-induced autophagy-related alterations, as evidenced by a reduction in the LC3-II/LC3-I ratio and decreased p62 accumulation, suggesting an alleviation of abnormal LC3-II accumulation and a partial restoration of autophagy homeostasis, rather than direct activation of autophagic flux. Moreover, propofol reversed the alterations in the AMPK/mTOR signaling by enhancing AMPK phosphorylation while suppressing mTOR activation. These observations indicate that propofol may deliver its neuroprotective function at least in part through modulation of the AMPK/mTOR signaling pathway, thereby alleviating neuroinflammation, oxidative stress, and apoptosis [22,23].

The outcomes of this research yield a meaningful understanding of the neuroprotective mechanisms by which propofol acts in HFD-induced brain injury. By modulating the AMPK/mTOR signaling pathway, propofol appears to mitigate neuroinflammation, oxidative stress, apoptosis, and autophagy-related alterations, ultimately improving cognitive function. These results highlight the promising clinical application of propofol for metabolism-linked neurodegenerative conditions.

However, several limitations should be acknowledged. First, the experiments were conducted in animal models, and translation of these findings to clinical practice requires further validation. Second, the precise molecular processes by which propofol modulates the AMPK/mTOR pathway remain to be fully elucidated. Third, only two propofol concentrations were evaluated in this study, providing a preliminary assessment of dose-related effects but limiting a comprehensive dose–response analysis. Future studies should explore the long-term effects of propofol treatment and examine additional dose gradients to further define the optimal therapeutic window.

Conclusion

In conclusion, our findings demonstrate that propofol exerts neuroprotective effects against HFD-induced brain injury by alleviating neuroinflammation, oxidative stress, apoptosis, and autophagy-related alterations, effects that may be associated with modulation of the AMPK/mTOR signaling pathway.

Availability of Data and Materials

The data used to support the findings of this study are available from the corresponding author upon request.

Author Contributions

SQY and KY conceived and designed the study. SQY and LL conducted the study. KY and QX contributed to data acquisition. QX and SQY analyzed the data. LL and QX interpreted the data. KY and QX drafted the manuscript. SQY, KY and LL reviewed and contributed to important editorial changes in the manuscript. All authors have read and approved the manuscript. All authors agreed to be accountable for all aspects of the work in ensuring that

questions related to the accuracy or integrity of any part of the work are appropriately investigated and resolved.

Ethics Approval and Consent to Participate

All experimental procedures were approved by the Institutional Animal Care and Use Committee of the Guangdong Provincial Medical Experimental Animal Center (IACUC Approval No. D202509-3) and were conducted in accordance with the ARRIVE guidelines.

Acknowledgment

Not applicable.

Funding

This research received no external funding.

Conflict of Interest

The authors declare no conflict of interest.

References

[1] Guillemot-Legris O, Muccioli GG. Obesity-Induced Neuroinflammation: Beyond the Hypothalamus. Trends in Neurosciences. 2017; 40: 237–253. https://doi.org/10.1016/j.tins.2017.02.005.

[2] Cavaliere G, Viggiano E, Trinchese G, De Filippo C, Messina A, Monda V, *et al*. Long Feeding High-Fat Diet Induces Hypothalamic Oxidative Stress and Inflammation, and Prolonged Hypothalamic AMPK Activation in Rat Animal Model. Frontiers in Physiology. 2018; 9: 818. https://doi.org/10.3389/fphys.2018.00818.

[3] Al-Kuraishy HM, Sulaiman GM, Mohsin MH, Mohammed HA, Dawood RA, Albuhadily AK, *et al*. Targeting of AMPK/MTOR signaling in the management of atherosclerosis: Outmost leveraging. International Journal of Biological Macromolecules. 2025; 309: 142933. https://doi.org/10.1016/j.ijbiomac.2025.142933.

[4] Chen F, Yi WM, Wang SY, Yuan MH, Wen J, Li HY, *et al*. A long-term high-fat diet influences brain damage and is linked to the activation of HIF-1α/AMPK/mTOR/p70S6K signalling. Frontiers in Neuroscience. 2022; 16: 978431. https://doi.org/10.3389/fnins.2022.978431.

[5] Zhu Q, Zhu YY, Wang WN. TRUSS inhibition protects against high fat diet (HFD)-stimulated brain injury by alleviation of inflammatory response. Biochemical and Biophysical Research Communications. 2019; 511: 41–48. https://doi.org/10.1016/j.bbrc.2019.01.058.

[6] Chen Y, Yu CY, Deng WM. The role of pro-inflammatory cytokines in lipid metabolism of metabolic diseases. International Reviews of Immunology. 2019; 38: 249–266. https://doi.org/10.1080/08830185.2019.1645138.

[7] Arruri V, Vemuganti R. Role of autophagy and transcriptome regulation in acute brain injury. Experimental Neurology. 2022; 352: 114032. https://doi.org/10.1016/j.expneurol.2022.114032.

[8] Liu F, Chen MR, Liu J, Zou Y, Wang TY, Zuo YX, *et al*. Propofol administration improves neurological function associated with inhibition of pro-inflammatory cytokines in adult rats after traumatic brain injury. Neuropeptides. 2016; 58: 1–6. https://doi.org/10.1016/j.npep.2016.03.004.

[9] Yu S, Liao J, Lin X, Luo Y, Lu G. Crucial role of autophagy in propofol-treated neurological diseases: a comprehensive review. Frontiers in Cellular Neuroscience. 2023; 17: 1274727. https://doi.org/10.3389/fncel.2023.1274727.

[10] Sun B, Ou H, Ren F, Huan Y, Zhong T, Gao M, *et al*. Propofol inhibited autophagy through Ca^{2+}/CaMKKβ/AMPK/mTOR pathway in OGD/R-induced neuron injury. Molecular Medicine. 2018; 24: 58. https://doi.org/10.1186/s10020-018-0054-1.

[11] Song W, Song C, Li L, Wang T, Hu J, Zhu L, *et al*. Lactobacillus alleviated obesity induced by high-fat diet in mice. Journal of Food Science. 2021; 86: 5439–5451. https://doi.org/10.1111/1750-3841.15971.

[12] Zhang HB, Tu XK, Chen Q, Shi SS. Propofol Reduces Inflammatory Brain Injury after Subarachnoid Hemorrhage: Involvement of PI3K/Akt Pathway. Journal of Stroke and Cerebrovascular Diseases. 2019; 28: 104375. https://doi.org/10.1016/j.jstrokecerebrovasdis.2019.104375.

[13] Guo XN, Ma X. The Effects of Propofol on Autophagy. DNA and Cell Biology. 2020; 39: 197–209. https://doi.org/10.1089/dna.2019.4745.

[14] Guan S, Sun L, Wang X, Huang X, Luo T. Propofol inhibits neuroinflammation and metabolic reprogramming in microglia *in vitro* and *in vivo*. Frontiers in Pharmacology. 2023; 14: 1161810. https://doi.org/10.3389/fphar.2023.1161810.

[15] Sahin K, Sahin E, Orhan C, Er B, Akoglan B, Ozercan IH, *et al*. The impact of magnesium biotinate and arginine silicate complexes on metabolic dysfunctions, antioxidant activity, inflammation, and neuromodulation in high-fat diet-fed rats. Clinical and Experimental Medicine. 2024; 24: 176. https://doi.org/10.1007/s10238-024-01434-9.

[16] Choi JW, Jo SW, Kim DE, Paik IY, Balakrishnan R. Aerobic exercise attenuates LPS-induced cognitive dysfunction by reducing oxidative stress, glial activation, and neuroinflammation. Redox Biology. 2024; 71: 103101. https://doi.org/10.1016/j.redox.2024.103101.

[17] Forouzanfar F, Read MI, Barreto GE, Sahebkar A. Neuroprotective effects of curcumin through autophagy modulation. IUBMB Life. 2020; 72: 652–664. https://doi.org/10.1002/iub.2209.

[18] Deneubourg C, Ramm M, Smith LJ, Baron O, Singh K, Byrne SC, *et al*. The spectrum of neurodevelopmental, neuromuscular and neurodegenerative disorders due to defective autophagy. Autophagy. 2022; 18: 496–517. https://doi.org/10.1080/15548627.2021.1943177.

[19] Zhu S, Wang S, Luo T. Exogenous galanin alleviates hepatic steatosis by promoting autophagy via the AMPK-mTOR pathway. Archives of Biochemistry and Biophysics. 2023; 744: 109689. https://doi.org/10.1016/j.abb.2023.109689.

[20] Liu Z, Jin Q, Yin J. Pachymic Acid A Alleviates Myocardial Injury in Acute Myocardial Infarction Mice by Regulating the AMPK/mTOR Pathway-Mediated Autophagy. Discovery Medicine. 2025; 37: 1630–1638. https://doi.org/10.24976/Discov.Med.202537199.142.

[21] Cheng X, Dai Y, Shang B, Zhang S, Lin L, Wu Q, *et al*. Danggui Shaoyao San and disassembled prescription: neuroprotective effects via AMPK/mTOR-mediated autophagy in mice. BMC Complementary Medicine and Therapies. 2024; 24: 298. https://doi.org/10.1186/s12906-024-04588-x.

[22] Ma J, Xiao W, Wang J, Wu J, Ren J, Hou J, *et al*. Propofol Inhibits NLRP3 Inflammasome and Attenuates Blast-Induced Traumatic Brain Injury in Rats. Inflammation. 2016; 39: 2094–2103. https://doi.org/10.1007/s10753-016-0446-8.

[23] Liu J, Ai P, Sun Y, Yang X, Li C, Liu Y, *et al*. Propofol Inhibits Microglial Activation *via* miR-106b/Pi3k/Akt Axis. Frontiers in Cellular Neuroscience. 2021; 15: 768364. https://doi.org/10.3389/fncel.2021.768364.